

# Organic & Biomolecular Chemistry

Volume 22  
Number 1  
7 January 2024  
Pages 1-186

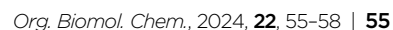
rsc.li/obc



ISSN 1477-0520

## COMMUNICATION

Stephen Neidle, Zoë A. E. Waller *et al.*  
QN-302 demonstrates opposing effects between i-motif  
and G-quadruplex DNA structures in the promoter of the  
S100P gene





*S100P* gene. All experiments were performed in 10 mM lithium cacodylate and 100 mM KCl. The G-quadruplex forming sequence was examined at pH 7.0 and the i-motif at between pHs 4.0 and 8.0. UV melting and annealing experiments showed that the G-rich sequence had a  $T_m$  of  $75.0 \pm 0.2$  °C and a  $T_a$  of  $73.3 \pm 0.7$  °C at pH 7.0 (Fig. S1†). This is consistent with our previous CD experiments indicating that the G-quadruplex structure formed would be highly stable under physiological conditions.<sup>17</sup> The complementary C-rich sequence had a  $T_m$  of  $45.4 \pm 0.6$  °C and a  $T_a$  of  $43.0 \pm 0.0$  °C at pH 5.5 (Fig. S2†). This  $T_m$  is similar to the melting temperature of other i-motifs of this length with three-cytosine long tracks at the same pH.<sup>23</sup> UV thermal difference spectroscopy on the C-rich sequence showed positive peaks at 240 and 265 nm and a negative peak at 295 nm (Fig. 2, left), consistent with i-motif structure.<sup>24</sup> Circular dichroism studies at acidic pH gave a spectrum with a positive peak at 288 nm and a negative peak at 260 nm, which is also consistent with an i-motif structure<sup>25</sup> (Fig. 2, right). The i-motif forming sequence was found to have a transitional pH ( $pH_T$ ) of 6.4, which indicates that this C-rich sequence can form an i-motif at near-neutral pH.<sup>23,26</sup>

QN-302 is one of the most potent G-quadruplex binding ligands reported to date with a  $K_d$  of 4.9 nM for the G-quadruplex forming sequence from hTERT.<sup>15</sup> It was previously shown to stabilise the G-quadruplex from the promoter region of *S100P* with  $\Delta T_m$  values of  $7.4 \pm 0.2$  °C at 10  $\mu$ M (1 eq.),  $17.0 \pm 0.1$  °C at 20  $\mu$ M (2 eq.) and  $20.0 \pm 1.3$  °C at 50  $\mu$ M (5 eq.) (Table 1).<sup>17</sup> These data indicates that QN-302 has a strong stabilising effect on the G-quadruplex structure formed.

We then focused in detail on the effects of QN-302 on the C-rich sequence from the *S100P* promoter.  $\Delta T_m$  values in the presence of QN-302 were determined in 10 mM lithium cacodylate, 100 mM KCl at pH 5.5, where the *S100P* sequence would be fully folded (Fig. 2). At 10  $\mu$ M (1 eq.) of QN-302 the  $\Delta T_m$  values were found to be  $-6.5 \pm 1.7$  °C,  $-14.3 \pm 0.1$  °C at 20  $\mu$ M (2 eq.) and  $-20.7 \pm 1.1$  °C at 50  $\mu$ M (5 eq.), demonstrating a dose-dependent destabilisation of i-motif structure by

**Table 1** Change in melting temperature ( $\Delta T_m$ ) of the *S100P* G-quadruplex and i-motif with QN-302 measured by CD melting experiments

[QN-302] $\mu$ M	$\Delta T_m$ (°C) <i>S100P</i> G – quadruplex <sup>17</sup>	$\Delta T_m$ (°C) <i>S100P</i> i – motif
10	$7.4 \pm 0.2$	$-6.5 \pm 1.7$
20	$17.0 \pm 0.1$	$-14.3 \pm 0.1$
50	$20.0 \pm 1.3$	$-20.7 \pm 1.1$



**Fig. 3** Representative CD melting experiments with 10  $\mu$ M *S100P* i-motif in 10 mM lithium cacodylate 100 mM KCl buffer (pH 5.5), and 0, 10, 20 or 50  $\mu$ M QN-302, as indicated.

QN-302 (Fig. 3, Table 1 and Fig. S4†). Other known G-quadruplex ligands such as berberine, BRACO-19, Phen-DC3, pyridostatin, RHPS4 and TmPyP4 have previously been shown to destabilise i-motifs, but to a lesser extent.<sup>27–29</sup> For example, BRACO-19 has a  $\Delta T_m$  values of  $-7.3 \pm 0.7$  °C for the i-motif forming sequence from the promoter region of the DAP gene<sup>28</sup> and  $-13.4 \pm 0.5$  °C for the i-motif from the human telomere. These  $\Delta T_m$  values are significantly smaller compared to our observations with QN-302. Di Porzio, Galli *et al.* have synthesised bis-triazolyl-pyridine derivatives that appear to have highly destabilising effects on the *c-Myc* and the hTelo i-motifs with  $\Delta T_m$  values of up to  $-29 \pm 1$  °C in one case. However, this destabilisation was achieved with double the number of ligand equivalents (10 molar equivalents) in phosphate buffer at pH 5.0.<sup>29</sup> These ligands did not have the same high stabilising effect on their respective G-quadruplexes as we observe with QN-302. To the best of our knowledge QN-302 is one of the most potent destabilising agents for i-motifs reported to date. Highly destabilising activity was also observed when QN-302 was tested against the i-motif forming sequences from the human genome including the telomeric sequence (hTelo), the insulin linked polymorphic region (ILPR) and the promoter region of DAP (Fig. S5–S7 and Table S1†).

To further investigate the destabilising effects of the *S100P* i-motif by QN-302 CD titrations were performed (Fig. 4). Upon addition of QN-302 at a concentration range from 0 to 110  $\mu$ M, the CD signal intensity at 288 nm was found to decrease in a dose-dependent fashion until a point at  $\sim 50$   $\mu$ M beyond which no further reduction in the ellipticity was observed. The



**Fig. 2** Left: thermal difference spectra of the C-rich i-motif forming *S100P* sequence: at 2.5  $\mu$ M in 10 mM lithium cacodylate and 100 mM KCl buffer at pH 5.5. Right: CD spectra of the C-rich *S100P* sequence at 10  $\mu$ M DNA in 10 mM lithium cacodylate and 100 mM KCl buffer at pH as indicated. Inset: corresponding plot of ellipticity at 288 nm at the different pHs to determine the transitional pH.





**Fig. 4** Left: CD titration of the C-rich *S100P* sequence (10  $\mu\text{M}$ ) and QN-302 (0–110  $\mu\text{M}$ ) in 10 mM lithium cacodylate and 100 mM KCl buffer at pH 5.5. Right: plot of ellipticity at 288 nm against QN-302 concentration and corresponding Hill 1 fitting.

decrease in the CD signal suggested ligand-dependent disruption of the *S100P* i-motif, consistent with unfolding of the structure to a single strand. This agrees with the CD melting experiments showing destabilisation. A plot of ellipticity against QN-302 concentration gave a sigmoidal-shaped curve (Fig. 4), indicative of a cooperative unfolding effect. By fitting the sigmoidal-shaped curves to the Hill 1 equation using Origin software, we obtained Hill coefficients ( $n$ ) of  $2.3 \pm 0.2$ . This reveals that the binding of QN-302 exhibits positive cooperativity ( $n > 1$ ) for the *S100P* i-motif. Additionally, the concentration of QN-302 that is required to reach 50% reduction of the molar ellipticity was determined to be  $31 \pm 4 \mu\text{M}$ . Analogous CD titration experiments with the G-quadruplex forming sequence showed no significant changes in topology (Fig. S3†). Indicating that the ligand is G-quadruplex stabilising and has both i-motif destabilising and unfolding properties. Taken together, the biophysical data illustrate the dynamic interplay of the two higher order DNA structures.

To further compare the affinity of QN-302 for the *S100P* i-motif and G-quadruplexes, UV titrations were performed (Fig. S8–S13 and Table S2†) and the dissociation constants ( $K_d$ ) were determined. The  $K_d$  for the G-quadruplex ( $K_d = 2.0 \pm 0.3 \mu\text{M}$ ) was found to be about six times lower than for the i-motif ( $K_d = 11.7 \pm 2.9 \mu\text{M}$ ), indicating that QN-302 has higher affinity for G-quadruplex compared to i-motif. This was not unexpected, given QN-302 was designed to target G-quadruplex structures.

Numerous studies have shown that high expression of the *S100P* gene is correlated with pancreatic cancer progression in humans.<sup>18–21</sup> The proposed mode of action involves the stabilisation of the G-quadruplex sequence in the promoter.<sup>17,22</sup> This stabilisation would inhibit transcription factor binding and the progression of RNA polymerase, resulting in direct downregulation of *S100P* gene expression at the transcriptional level analogous to other ligands such as pyridostatin.<sup>16,17,30</sup> In this study we have further examined the mechanistic details of QN-302 interacting with the higher-order structures that can be formed in this promoter region of the *S100P* gene and in particular have examined the potential role of the i-motif formed by the C-rich strand. QN-302 has a strong destabilising effect on the *S100P* i-motif as it is illustrated by CD melting

and titration experiments. Therefore, QN-302 by stabilizing the G-quadruplex structure and destabilizing the i-motif structure, has a dual role and may exert a synergistic effect on the inhibition of transcription of the *S100P* gene. Ligand-induced G-quadruplex stabilization inhibits gene expression whereas stabilization of i-motifs could activate transcription.<sup>31,32</sup> This highlights the importance of evaluating the effects of a compound on both the i-motifs and the G-quadruplexes potentially formed from a duplex region of appropriate sequence. This is particularly important given the fact that G-quadruplex and i-motif formation in cells are interdependent.<sup>33</sup> In the case of *S100P*, there is biological evidence that QN-302 can switch off gene expression<sup>17</sup> which may be a consequence of both the stabilisation of the G-quadruplex and the destabilisation of the i-motif. This suggests how these two alternative structures operate together in the *S100P* promoter.

The findings reported here demonstrate that QN-302 both strongly stabilizes the *S100P* promoter G-quadruplex and strongly destabilizes the complementary i-motif *in vitro*. These data are consistent with and supportive of previous conclusions<sup>16</sup> that QN-302 down-regulates the expression of numerous cancer-related genes by pan-quadruplex targeting. This is particularly important given the recent analysis of TCGA PanCancer Atlas PDAC datasets that indicate poor prognosis in patients with high *S100P* expression.<sup>34</sup> QN-302 exhibits exceptional combined synergistic effects compared to many other G-quadruplex and i-motif interacting compounds. Overall, this work further emphasises the importance of considering these two alternative DNA structures as one dynamic system and as one target.

## Data availability

Data is available on Figshare: [10.6084/m9.figshare.24476551](https://figshare.com/data/articles/10.6084/m9.figshare.24476551).

## Author contributions

S. N. and Z. A. E. W. conceived the study, E. A., D. G. and Z. A. E. W. designed the experiments E. A. and D. G. performed the experiments E. A., D. G., S. N. and Z. A. E. W. wrote the paper, contributed to the manuscript revision, and approved the final version.

## Conflicts of interest

S. Neidle is a paid consultant and Advisory Board member of Qualigen Inc.

## Acknowledgements

D. G. is supported by the Biotechnology and Biological Sciences Research Council grant BB/W001616/1.



## References

- 1 A. Siddiqui-Jain, C. L. Grand, D. J. Bearss and L. H. Hurley, *Proc. Natl. Acad. Sci. U. S. A.*, 2002, **99**, 11593–11598.
- 2 J. L. Huppert and S. Balasubramanian, *Nucleic Acids Res.*, 2007, **35**, 406–413.
- 3 S. Balasubramanian, L. H. Hurley and S. Neidle, *Nat. Rev. Drug Discovery*, 2011, **10**, 261–275.
- 4 K. Shin, N. A. Chapman, M. Sarker, C. Kenward, S. K. Huang, N. Weatherbee-Martin, A. Pandey, D. J. Dupré and J. K. Rainey, *Biochim. Biophys. Acta, Gen. Subj.*, 2017, **1861**, 1901–1912.
- 5 S. Lago, M. Nadai, F. M. Cernilogar, M. Kazerani, H. Domínguez Moreno, G. Schotta and S. N. Richter, *Nat. Commun.*, 2021, **12**, 3885.
- 6 S. L. Brown and S. Kendrick, *Pharmaceuticals*, 2021, **14**, 96.
- 7 K. L. Irving, J. J. King, Z. A. E. Waller, C. W. Evans and N. M. Smith, *Biochimie*, 2022, **198**, 33–47.
- 8 S. Neidle, *J. Med. Chem.*, 2016, **59**, 5987–6011.
- 9 H. Xu and L. H. Hurley, *Bioorg. Med. Chem. Lett.*, 2022, **77**, 129016.
- 10 E. Mendes, I. M. Aljnadi, B. Bahls, B. L. Victor and A. Paulo, *Pharmaceuticals*, 2022, **15**, 300.
- 11 E. Ruggiero and S. N. Richter, *Bioorg. Med. Chem. Lett.*, 2023, **79**, 129085.
- 12 A. Heine, S. Juranek and P. Brossart, *Mol. Cancer*, 2021, **20**, 52.
- 13 M. Micco, G. W. Collie, A. G. Dale, S. A. Ohnmacht, I. Pazitna, M. Gunaratnam, A. P. Reszka and S. Neidle, *J. Med. Chem.*, 2013, **56**, 2959–2974.
- 14 C. Marchetti, K. G. Zyner, S. A. Ohnmacht, M. Robson, S. M. Haider, J. P. Morton, G. Marsico, T. Vo, S. Laughlin-Toth, A. A. Ahmed, G. Di Vita, I. Pazitna, M. Gunaratnam, R. J. Besser, A. C. G. Andrade, S. Diocou, J. A. Pike, D. Tannahill, R. B. Pedley, T. R. J. Evans, W. D. Wilson, S. Balasubramanian and S. Neidle, *J. Med. Chem.*, 2018, **61**, 2500–2517.
- 15 T. Vo, S. Oxenford, R. Angell, C. Marchetti, S. A. Ohnmacht, W. D. Wilson and S. Neidle, *ACS Med. Chem. Lett.*, 2020, **11**, 991–999.
- 16 A. A. Ahmed, R. Angell, S. Oxenford, J. Worthington, N. Williams, N. Barton, T. G. Fowler, D. E. O'Flynn, M. Sunose, M. McConville, T. Vo, W. D. Wilson, S. A. Karim, J. P. Morton and S. Neidle, *ACS Med. Chem. Lett.*, 2020, **11**, 1634–1644.
- 17 A. A. Ahmed, W. Greenhalf, D. H. Palmer, N. Williams, J. Worthington, T. Arshad, S. Haider, E. Alexandrou, D. Guneri, Z. A. E. Waller and S. Neidle, *Molecules*, 2023, **28**, 2452.
- 18 F. Prica, T. Radon, Y. Cheng and T. Crnogorac-Jurcevic, *Am. J. Cancer Res.*, 2016, **6**, 562–576.
- 19 Y. Wu, Q. Zhou, F. Guo, M. Chen, X. Tao and D. Dong, *Front. Oncol.*, 2021, **11**, 711180.
- 20 N. Ideno, Y. Mori, M. Nakamura and T. Ohtsuka, *Diagnostics*, 2020, **10**, 1056.
- 21 W. Zou, L. Li, Z. Wang, N. Jiang, F. Wang, M. Hu and R. Liu, *Bioengineered*, 2021, **12**, 9006–9020.
- 22 A. Gibadulinova, I. Oveckova, S. Parkkila, S. Pastorekova and J. Pastorek, *Oncol. Rep.*, 2008, **20**, 391–396.
- 23 E. P. Wright, J. L. Huppert and Z. A. E. Waller, *Nucleic Acids Res.*, 2017, **45**, 2951–2959.
- 24 J.-L. Mergny, J. Li, L. Lacroix, S. Amrane and J. B. Chaires, *Nucleic Acids Res.*, 2005, **33**, e138–e138.
- 25 J. Kypr, I. Kejnovská, D. Renciuik and M. Vorlícková, *Nucleic Acids Res.*, 2009, **37**, 1713–1725.
- 26 J. Zhou, C. Wei, G. Jia, X. Wang, Z. Feng and C. Li, *Mol. Biosyst.*, 2010, **6**, 580–586.
- 27 A. Pagano, N. Iaccarino, M. A. S. Abdelhamid, D. Brancaccio, E. U. Garzarella, A. Di Porzio, E. Novellino, Z. A. E. Waller, B. Pagano, J. Amato and A. Randazzo, *Front. Chem.*, 2018, **6**, 281.
- 28 M. A. S. Abdelhamid, A. J. Gates and Z. A. E. Waller, *Biochemistry*, 2019, **58**, 245–249.
- 29 A. Di Porzio, U. Galli, J. Amato, P. Zizza, S. Iachettini, N. Iaccarino, S. Marzano, F. Santoro, D. Brancaccio, A. Carotenuto, S. De Tito, A. Biroccio, B. Pagano, G. C. Tron and A. Randazzo, *Int. J. Mol. Sci.*, 2021, **22**, 11959.
- 30 J. Spiegel, S. M. Cuesta, S. Adhikari, R. Hänsel-Hertsch, D. Tannahill and S. Balasubramanian, *Genome Biol.*, 2021, **22**, 117.
- 31 H. J. Kang, S. Kendrick, S. M. Hecht and L. H. Hurley, *J. Am. Chem. Soc.*, 2014, **136**, 4172–4185.
- 32 S. Kendrick, H. J. Kang, M. P. Alam, M. M. Madathil, P. Agrawal, V. Gokhale, D. Yang, S. M. Hecht and L. H. Hurley, *J. Am. Chem. Soc.*, 2014, **136**, 4161–4171.
- 33 J. J. King, K. L. Irving, C. W. Evans, R. V. Chikhale, R. Becker, C. J. Morris, C. D. Peña Martinez, P. Schofield, D. Christ, L. H. Hurley, Z. A. E. Waller, K. S. Iyer and N. M. Smith, *J. Am. Chem. Soc.*, 2020, **142**, 20600–20604.
- 34 K. Srivastava, K. E. Lines, D. Jach and T. Crnogorac-Jurcevic, *Oncogene*, 2023, DOI: [10.1038/s41388-023-02851-y](https://doi.org/10.1038/s41388-023-02851-y).

